Modelling Acoustic Excitation of High Frequency Combustion Instability Experiments

S. Beinke ,**, J. Hardi*, M. Oschwald*, and B. Dally***
**German Aerospace Center (DLR) - Institute of Space Propulsion*
Lampoldshausen, D-74239 Hardthausen, Germany
***The University of Adelaide – School of Mechanical Engineering*
Adelaide 5005, South Australia, Australia

Abstract

This work is concerned with the development of a numerical model to predict combustion instability phenomena in a high pressure combustion chamber. The model is being developed to simulate an experimental combustion chamber operated at DLR Lampoldshausen that is acoustically excited using a secondary nozzle and siren wheel system. The experimental data correlates flame response to an acoustic field. Experimental data from cold flow experiments are analysed to study the nature of the acoustic system without having to consider heat release and other processes associated with combustion. The different numerical schemes used to represent the excitation system are investigated.

1 Introduction

Combustion instabilities refer to a coupling between acoustic and combustion processes inside combustion chambers. Acoustic pressure fluctuations propagate throughout a combustion chamber and interact with the combustion processes occurring therein. Under certain conditions the frequency of the fluctuations may be such that mutual reinforcement occurs, producing self-sustaining oscillations, referred to as combustion instabilities. If unimpeded, the amplitude of the instability fluctuations may grow to levels where it affects the operation and compromises the structure of the combustion chamber. Combustion instabilities reduce the lifetime and reliability of rocket engine combustion chambers and have the potential to cause premature failure of the rocket engine, usually resulting in loss of a rocket mission.

High frequency combustion instabilities, occurring at frequencies greater than 1000 Hz, are the least understood and most damaging type of instability. At high frequencies the acoustic behaviour is attributed to the resonant modes of the combustion chamber volume. The mechanisms which determine how combustion processes interact with and support acoustic disturbances at these frequencies are not yet understood. This is in part due to the complexity of the problem, as various combustion processes such as atomisation, mixing, and combustion occur simultaneously inside a combustion chamber. To investigate combustion instabilities requires consideration of each of the aforementioned processes and their interaction with high frequency acoustic processes. Various experimental investigations have been completed and guidelines to prevent instability behaviour have been devised. An extensive summary of combustion instability research and treatment techniques was compiled in 1972 [9]. Further guidelines to ensure rocket engine combustion chambers are free from combustion instabilities have been published by Priem [18]. Nevertheless, extensive ground testing of the engine over its operational envelope remains the only available method for ensuring an engine is free from combustion instabilities.

Ground testing of rocket engine systems is expensive and typically does not occur until the later stages of development. If instabilities are discovered additional time and costs must be added to treat the instability. Additional ground testing of the treated engine may then also be needed to certify its stability. The ability to accurately predict combustion instabilities during the design phase would reduce the need for ground testing and the risks associated with rocket engine development. Numerical modelling methods are being developed by a number of research groups in the hope of fulfilling this role and provide further insight into combustion instability experiments.

This paper examines a nozzle and siren wheel acoustic excitation system used in combustion instability experiments. Variations of this system have been used during different high frequency combustion instability experiments with sub-scale combustion chambers. The BKH combustion chamber operated at DLR Lampoldshausen is the focus of the current work. Results from BKH combustor experiments with excitation are presented. Numerical boundary conditions to represent the acoustic excitation system for simulations of the BKH experiment are described and implemented to simulate excitation at the first transverse (1T) mode frequency. This work is a continuation of previous work [1] which examined excitation at off resonance conditions.

1.1. Acoustic Excitation Systems

The purpose of an acoustic excitation system for combustion instability research is to produce an acoustic disturbance within the combustion chamber. As this disturbance propagates throughout the combustion chamber it interacts with a study element. The response of the study element to the applied disturbance is then observed. The frequency of the disturbance produced by the system can be controlled to deliberately excite the resonant modes of the combustion chamber. Experimental combustion chambers that use these systems are typically naturally stable and are used to study the effect of the acoustic disturbance on combustion processes for various operating conditions. Instabilities in naturally unstable combustion chambers are uncontrolled, which makes characterisation of the acoustic field more challenging.

Various methods of artificially exciting combustion chambers have been used. In ambient and cold flow operating conditions, electronic actuator acoustic excitation systems may be used. Chehroudi et al. [2, 3] used a piezo-siren acoustic excitation system to study nitrogen jets at sub- and super-critical nitrogen pressure conditions under acoustic excitation. Electronic actuators have not been used for high frequency combustion instability research during hot fire operation of combustion chambers.

To acoustically excite combustion instability experiments under hot fire conditions it has so far been easier to use a system that modulates the flow into or out of the combustion chamber. The first example of such a system was developed by Leocourt and Foucaud [12]. They successfully produced a periodic acoustic disturbance by modulating the throat area of a nozzle attached to the chamber. A rotating toothed wheel was aligned such that the teeth cover nozzle throat. As the wheel rotated the flow through the nozzle was periodically interrupted causing a rise in pressure which then propagated from the nozzle back into the chamber. Hardi et al. [8] lists and describes modern examples of high frequency combustion instability experiments conducted using similar nozzle and siren wheel systems; the Common Research Combustor (CRC) operated by the DLR and the French National Center for Scientific Research (CNRS), the multi-injector combustor (MIC) and very high amplitude modulator (VHAM) operated by the French Aerospace Lab (ONERA) and CNRS [14], and the BKH combustion chamber operated by DLR.

The disturbance produced by nozzle and siren wheel system has not been studied in detail. The systems are intended to produce a smooth sinusoidal disturbance, but this has not been observed experimentally. Limited experimental data has been collected to describe the flow conditions in the vicinity of a nozzle and siren wheel system. Further analysis of experimental data requires understanding of the acoustic disturbance perturbing the flame or study element. Determining the actual amplitude and profile of the disturbance is therefore critical.

1.2. Methods of Representing the Acoustic Excitation System

Simulation of high frequency combustion instabilities requires consideration of the coupling between acoustics and heat release. When moving beyond simplified cases an analytical approach is not possible due to the number of complex processes affecting heat release, such as atomisation, mixing, and combustion, which are also affected by acoustic processes. The increasing computational power and resources available today has led to the use of flow solvers to simulate the flow field and combustion. The acoustic processes are then calculated by either a separate acoustic solver, or by the flow solver itself. The method by which the acoustic disturbance is imposed upon the model is dependent on the overall approach taken.

Nicole and Habiballah [15] and Laroche et al. [10] used a flow solver to model both the flow field and acoustics. Acoustic disturbances were imposed by superimposing an acoustic disturbance upon an initial flow field solution and observing its decay during transient simulations. This method allowed the damping of the chamber to be assessed, but cannot be applied to a continuously driven system.

Schmid and Sattelmayer [20, 21] employ an acoustics solver coupled to a flow solver. The flow solver is used to simulate single injection elements. Acoustic disturbances are imposed on the injection elements by applying a calculated mass flow across the computational domain. The mass flow is calculated by the acoustics solver, such that it matches the acoustic disturbance at the location of the injection element. The response of the element to the acoustic disturbance calculated by the flow solver is then reported to the acoustics solver. As the computational domain of the flow solver is reduced this method is numerically less expensive when simulating a chamber with a large number of injection elements.

Rey et al. [19] describe a method whereby transverse acoustic disturbances acting upon a reduced computational domain of multiple injection elements by imposing a flow velocity into and out of the domain at the boundaries. Mery et al. [12] and Hakim et al. [5] have used this method to model the MIC with VHAM excitation producing a transverse disturbance across the injection region using a flow solver.

Nicole [15] and Hakim et al. [5] have also simulated the entire VHAM geometry with an acoustic excitation system. The influence of the acoustic excitation system was approximated by a sinusoidal pressure or mass flow at the boundary of the nozzle during transient simulations.
The aforementioned methods, when applied to a combustion chamber that uses an acoustic excitation system, require various assumptions. A validated methodology that required fewer assumptions about the nature of the acoustic disturbance could be applied with greater confidence and possibly used to inform and investigate the validity of the assumptions required for other methods.

2 Experimental Setup

The BKH combustor, shown in Figure 1, is used for high frequency combustion instability experiments. BKH operates at pressures ranging from 40 bar (sub-critical oxygen pressure) to 60 bar (super-critical oxygen pressure) using cryogenic oxygen and hydrogen propellants. The combustion chamber features a rectangular geometry with windows located on each side for optical access to the injection zone, and a nozzle and siren wheel for excitation. The combustion chamber volume is 305 mm long, 50 mm wide and 200 mm high. The rectangular geometry was designed to match the resonant mode frequencies of full-scale upper-stage rocket engines. BKH experiments are conducted at the European Research and Technology test Facility P8 for cryogenic rocket engines at DLR Lampoldshausen. Additional BKH information can be found in Ref. [6, 7 & 8].

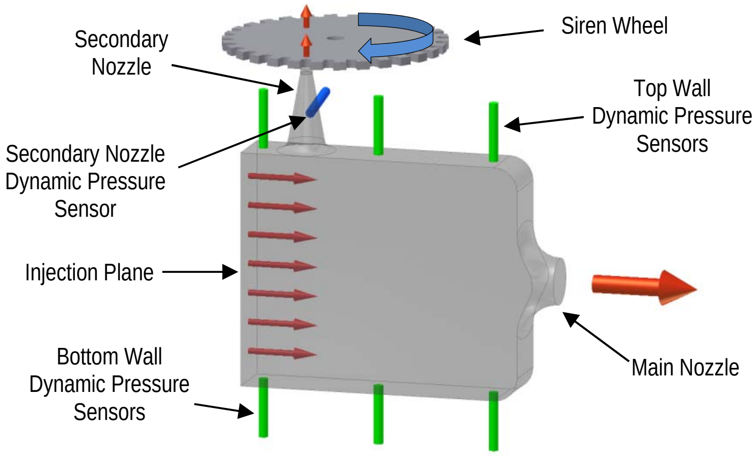

Figure 1: Concept diagram of the BKH chamber and excitation system

The BKH excitation system consists of a secondary nozzle located in the top wall of the chamber and an siren wheel. The secondary nozzle is oriented perpendicular to the flow direction to favour excitation of transverse acoustic modes. The secondary nozzle throat area is approximately 16 times smaller than the main nozzle throat area. The rotational velocity of the siren wheel is controlled during a test to ramp through a range of frequencies and excite the resonant modes of the chamber. With the excitation system, BKH experiments have recorded acoustic pressure fluctuation amplitudes greater than 9% mean chamber pressure when exciting at the resonant frequency of the chamber.
Cold flow tests are completed primarily to test new experimental hardware. During a cold flow test only hydrogen gas is injected into the chamber and no combustion occurs. Therefore cold flow tests provide an opportunity to study the chamber acoustics without the influence of combustion processes.

3 Experimental Results

BKH cold flow tests have been conducted with operation of the acoustic excitation system. The frequency of the acoustic disturbance applied by the excitation system is ramped during the test to observe the response of the chamber to a range of frequencies. Dynamic pressure data is recorded from sensors located in the walls of the chamber and a sensor located in the secondary nozzle. Figure 2 shows a spectrogram of dynamic pressure data recorded from a sensor in the bottom wall of the combustion chamber opposite to the secondary nozzle. Faint horizontal bands show the frequencies of the resonant modes of the combustion chamber which are weakly excited over the duration of the test.

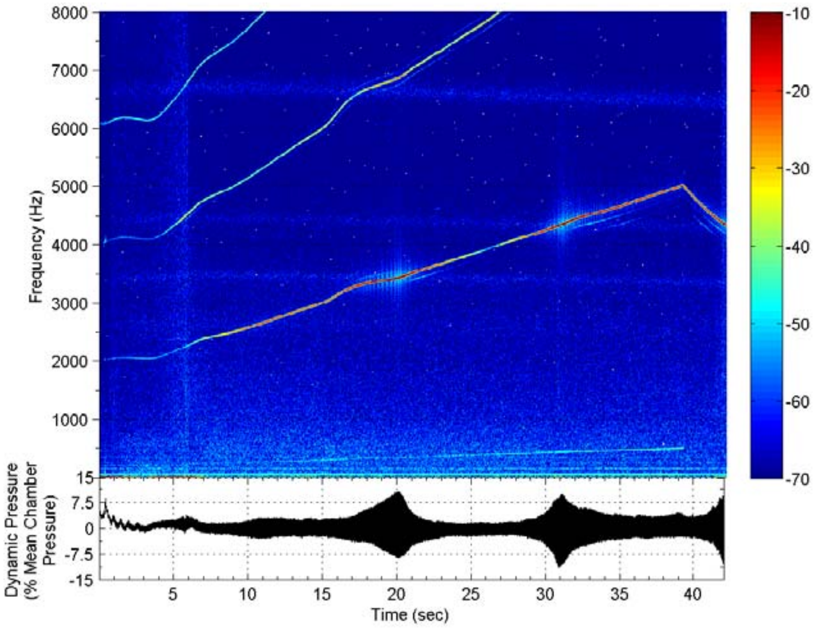

Figure 2: Spectrogram of dynamic pressure sensor data from BKH cold flow experiment (top) and dynamic pressure data (bottom)

The frequency of the acoustic excitation system disturbance is clearly visible in Figure 2 as it steadily ramps from a starting frequency of 2 kHz at 4 seconds to 5 kHz at 39 seconds. A noticeable increase in the amplitude of the acoustic disturbance is observed when the excitation frequency corresponds to a resonant frequency of the combustion chamber. This occurs at 20 seconds when the excitation frequency corresponds to the 1T mode resonant frequency of the chamber. Overtones of the excitation frequency are also visible at double and triple the excitation frequency. These overtones indicate that the disturbance produced by the excitation system is not an ideal sinusoidal profile but is also producing disturbances at a number of frequencies.

Figures 3 and 4 shows dynamic pressure data recorded during excitation of the 1T mode in greater detail. Figure 3 shows the disturbance observed in the secondary nozzle. The profile of the disturbance is evidently non-linear, featuring a very steep profile. The disturbance is also not symmetrical about 0. The high pressure part of the cycle appears to be smooth, while the low pressure part of the cycle remains relatively constant for one third of the cycle. It also features a small secondary peak, which belongs to the first overtone of the excitation frequency. Figure 4 shows the secondary nozzle in comparison to other sensors located in the combustion chamber. The sensors in the top of the chamber are in phase with the secondary nozzle sensor, while the sensors located on the bottom wall of the chamber are 180 degrees out of phase. This is characteristic of the 1T mode in the combustion chamber.

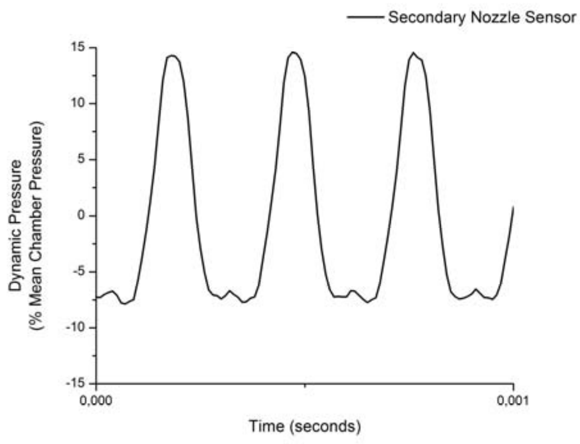

Figure 3: Experimental data recorded by the secondary nozzle sensor during 1T mode excitation

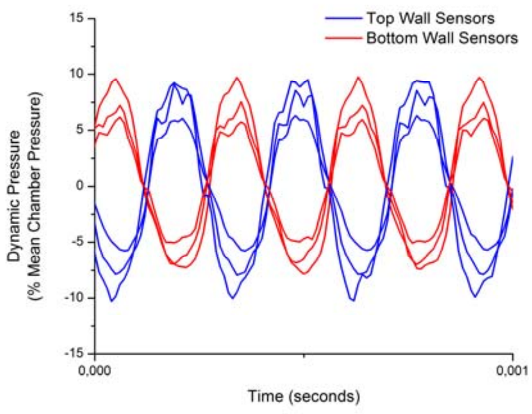

Figure 4: Experimental data recorded from wall mounted sensors during 1T mode excitation

Pressure data recorded during a period of off-resonance excitation of 3 kHz is shown in Figures 5 and 6. Figure 5 shows that at off resonance conditions the disturbance produced by the secondary nozzle features a different profile to that at the 1T mode frequency. The disturbance is again unsymmetrical, and the ratio of the amplitude of the primary to the secondary peak has decreased. Figure 6 shows data from other pressure sensors mounted on the walls of the combustion chamber during off resonance excitation. When not exciting at the resonant frequency, the wall sensor data shows that the pressure disturbance produces a structure where the sensors at the top and bottom of the chamber remain out of phase, exhibiting a phase relationship similar to a 1T mode. However the amplitudes recorded at neighbouring sensor positions do not correspond to a 1T mode structure and a range of pressure amplitudes are seen at different locations within the chamber. Part of the disturbance imposed on the chamber has begun to support 1T mode oscillations within the chamber; however the chamber is also being excited at other frequencies which interfere and prevent a 1T mode with significant amplitudes from being established.

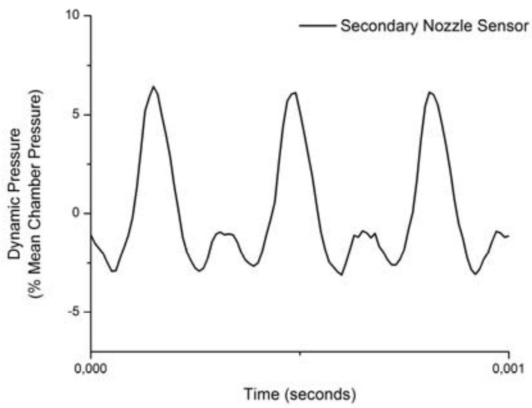

Figure 5: Experimental data recorded the secondary nozzle sensor during off resonance excitation

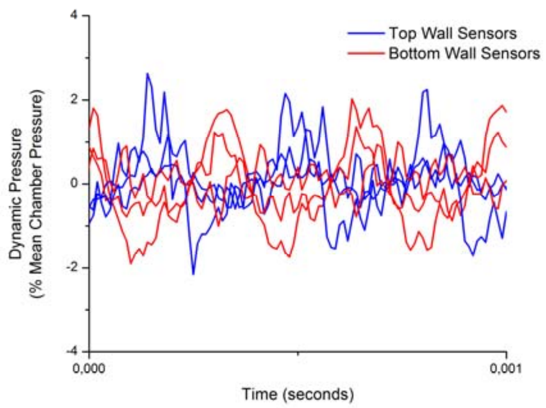

Figure 6: Experimental data recorded from wall mounted sensors during off resonance excitation

4 Numerical Approach

Acoustic disturbances inside the BKH chamber are generated by the interrupted flow through the secondary nozzle. To model the transfer of fluid motion into acoustic pressure, the DLR Tau-code flow solver was selected to simulate both flow and acoustic processes. Simulation of the physical excitation system by modelling the components in detail is outside the scope of the current work. Instead, different boundary conditions are implemented at the secondary nozzle exit plane boundary and the resulting acoustic disturbance is compared with BKH experimental results to determine the best match. The boundary conditions are applied to perturb a pre-calculated simulation of the steady state flow field in the BKH chamber. The approach is being developed for cold flow operating conditions in order to study the acoustic properties of the BKH chamber in detail. In the future the method and boundary conditions will be applied to simulate hot fire BKH experiments under acoustic excitation.

The DLR Tau-code is a hybrid structured/unstructured second-order finite-volume flow solver for the compressible Euler and Navier-Stokes equations in the integral form. It has been validated for a range of steady and unsteady flow cases [4]. Turbulence models ranging from RANS one- and two-equation models to detached and large eddy simulations have been implemented in Tau.

Karl and Leudeke [10] validated the Tau-code for acoustic damping cavities. They employed the AUSMPUP upwind solver which is an extension of the AUSM+ scheme. A Jameson-type dual time stepping scheme was used to perform unsteady RANS calculations. The same numerical method is used for the current work.

In this paper, results produced by numerically exciting a cold flow model of the BKH chamber at the 1T frequency using two different methods are presented and discussed. The boundary conditions are used to represent the siren excitation at the 1T mode frequency of 3.3 kHz. This frequency was determined from experimental observation and previous analysis of the BKH chamber [8].

4.1. Description of Boundary Conditions

Two different boundary condition methodologies to numerically represent the influence of the siren wheel have been examined. Transient computations are begun from the previously computed, unperturbed flow field solution. The boundary conditions which are applied to the secondary nozzle exit plane boundary are described in the following sections.

Open/Closed Boundary

For the open/closed boundary condition the secondary nozzle exit plane is alternated between an outflow, representing the nozzle being open, and a solid wall, representing the nozzle being blocked by a tooth of the excitation wheel. The controlling parameter for this approach is the ratio of time per cycle the boundary is open or closed. For this work, the boundary condition was alternated such that the nozzle is open and closed for equal periods of time. When the nozzle is open it is assumed to be venting to a volume at atmospheric pressure. In the future this approach may be further tuned by modifying the boundary condition to prevent the nozzle from being entirely closed, representing the small clearance between the excitation wheel teeth and the secondary nozzle throat, and by staggering the change in boundary condition to represent the nozzle exit gradually being covered and uncovered by the teeth of the excitation wheel.

Sinusoidal Pressure Boundary

For the sinusoidal pressure boundary condition the secondary nozzle exit plane is prescribed as an outflow condition. The pressure prescribed at this boundary, P_{out}, is then modified to reflect the rise in pressure produced by the excitation wheel interrupting the flow through the secondary nozzle. The pressure is modulated assuming a sinusoidal pressure disturbance by Equation 1.

$$P_{out} = P_{start} + P_d(1 - \cos(\omega \times t)) \quad \textbf{(1)}$$

The start pressure, P_{start}, was set to ambient pressure to match the initial unperturbed conditions where the nozzle is open. The disturbance pressure, P_d, was set to just over half the mean chamber pressure. Therefore the prescribed pressure fluctuates between ambient pressure corresponding to a fully open nozzle, and slightly more than the mean chamber pressure representing the nozzle being blocked.
This approach is based on the assumption that the secondary nozzle is not completely blocked by the siren wheel at any point. Therefore the flow through the nozzle is never completely halted. The amplitude of the disturbance P_d may be controlled in the future to better match experimentally observed values.

5 Numerical Results

5.1. Unperturbed BKH Solution

A 3D RANS simulation of a BKH cold flow experiment was calculated using the DLR Tau code. The result of this simulation is shown in Figure 7.

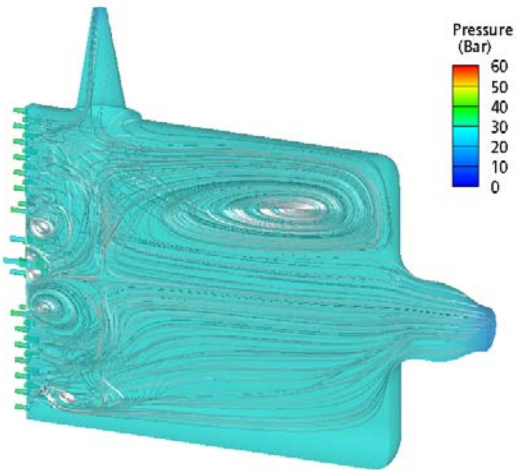

Figure 7: Unperturbed BKH cold flow simulated flow field showing pressure contours at the boundaries of the numerical domain and streamlines from planes at 5, 10, and 15 mm in the Z-direction.

Hydrogen at ambient temperature is injected into the chamber through the primary and secondary injectors. One of the roles of the secondary injectors is to reduce recirculation near the injection plane of the BKH chamber. A symmetry boundary condition is applied to take advantage of the vertical symmetry in the BKH combustion chamber and reduce the size of the computational domain. The resulting flow field features some recirculation zones about the primary injectors and a large recirculation zone located in the top half of the combustion chamber. Ninety two percent of the mass flow entering the chamber exits through the main nozzle while the rest of the mass flow exits via the secondary nozzle at the top of the chamber.

5.2. Perturbed BKH Results

Comparison of Mode Structure

Correctly capturing the structure of the excited 1T mode is important for future investigations and analysis as it determines the spatial distribution of the acoustic disturbance. In previous BKH studies [7], the 1T-mode structure was assumed to be similar to a two-dimensional Eigenmode solution to the linear acoustic wave equation, as shown in Figure 8. The Eigenmode solution has a pressure nodal line which closely follows the horizontal axis of the chamber. A better estimate of the nodal line position and the acoustic field distribution near the primary injectors would benefit analysis of BKH experimental results.

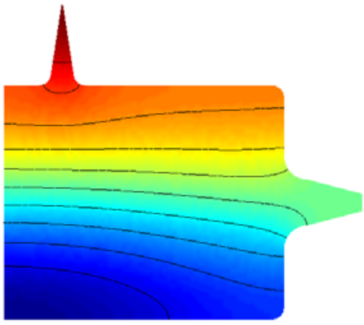

Figure 8: Eigenmode solution of the 1T mode in a 2D model of the BKH combustion chamber

Instantaneous pressure fields from simulations using each of the boundary conditions described in Section 4.1 have been extracted and are shown in Figures 9 and 10. The instantaneous pressure fields were extracted from periods of high amplitude after a limit cycle had been reached.

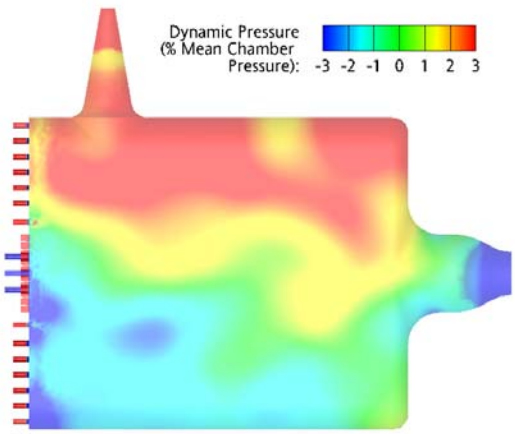

Figure 9: Instantaneous pressure field extracted from numerical results after 3.5 ms of 1T-mode excitation using the open/closed boundary condition

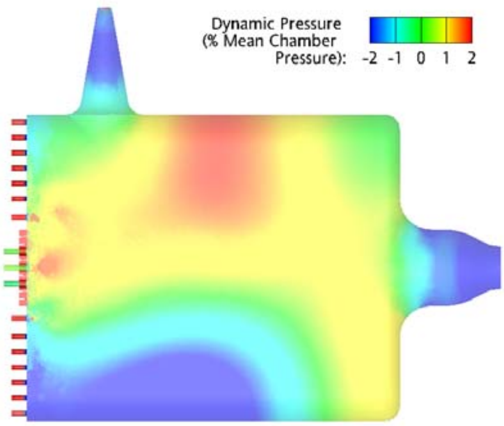

Figure 10: Instantaneous pressure field extracted from numerical results after 4.975 ms of 1T-mode excitation using the sinusoidal pressure boundary condition

Figure 9 shows that the open/closed boundary condition produces a mode structure where the pressure oscillations are out of phase in the top and bottom of the chamber, as is expected for the 1T mode. However, the pressure distribution does not steadily change from one side of the chamber to the other, as predicted by the Eigenmode solution. Figure 10, which was extracted from a simulation using the sinusoidal pressure boundary condition, also

shows a distribution where the pressure in the top and bottom of the chamber are out of phase. This distribution features less chaotic pressure gradients throughout the combustion chamber compared to that in Figure 9. However, it does not resemble a 1T mode in the longitudinal direction. These results show that the nature of the disturbance applied at the secondary nozzle can affect the structure of the excited acoustic mode.
The results of each simulation have been post-processed for comparison with experimental data. Pressure data are extracted from periods after the limit cycle had been reached at the locations of the pressure sensors used in BKH experiments. The results are presented for each boundary condition in the following sections.

Open/Closed Boundary

The unperturbed BKH solution was perturbed at the 1T mode frequency by applying the open/closed boundary condition to represent acoustic excitation for a number of excitation periods. The disturbance was found to reach a limit cycle after approximately 3ms of simulated time. Figure 11 shows the simulated secondary nozzle pressure sensor measurement and a representation of the state of the secondary nozzle boundary during this period. This data is comparable with the experimental data shown in Figure 3. The open/closed boundary condition produces a very sharp peak due to the sudden change that is imposed on the secondary nozzle boundary. This pressure peak reaches the secondary nozzle sensor after a brief delay. The amplitude of the pressure disturbance in the secondary nozzle is larger than that observed experimentally. A second spike in pressure occurs shortly after the nozzle opens. The pressure also begins to rise a second time after the nozzle has been open for a short time.

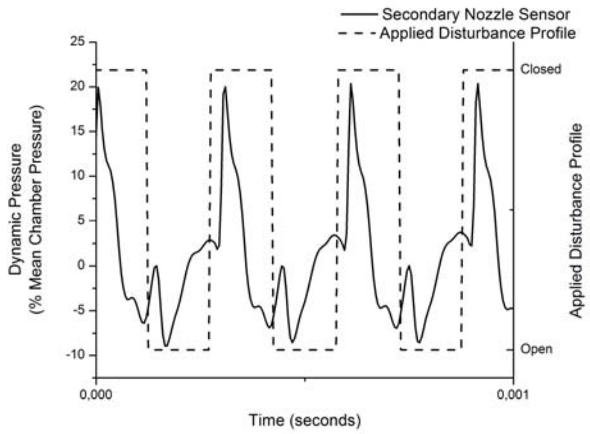

Figure 11: Extracted pressure data from the secondary nozzle sensor position during 1T mode excitation and the applied disturbance profile for the open/closed boundary condition.

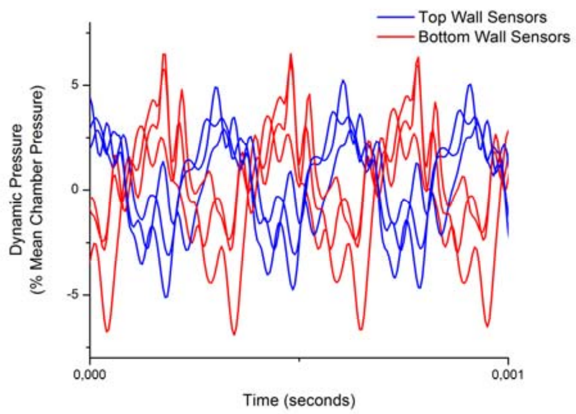

Figure 12: Extracted pressure data from the chamber wall sensor position during 1T mode excitation for the open/closed boundary condition.

Figure 12 shows simulated pressure data extracted from the wall mounted pressure sensor locations in the top and bottom of the chamber. This plot is comparable to the experimental results shown in Figure 4. The top and bottom wall sensors are out of phase which is indicative of a 1T mode structure. The simulated data contains considerably more noise and higher frequencies than the experimental results. The amplitudes of the simulated data are also lower than those observed experimentally at the 1T mode. The amplitudes are instead closer to the amplitudes observed during off resonance excitation. The open/closed boundary condition produces a very steep-fronted disturbance which has stronger associated overtones. Thus this currently crude implementation of such a boundary condition method excites multiple excitation frequencies which may be interfering and reducing the amplitude of the 1T mode.

Sinusoidal Pressure Boundary

The steady BKH solution was also perturbed at the 1T excitation frequency using the sinusoidal pressure boundary condition. The amplitude of the numerical disturbance reached its maximum amplitude after approximately 2.8 ms of simulated time. Figure 13 shows the simulated secondary nozzle pressure sensor amplitude and a representation of the pressure applied to the secondary nozzle boundary during the simulation. The disturbance recorded at the secondary nozzle pressure sensor position has a smooth profile and there is a slight delay between when the disturbance is applied at the nozzle boundary and when it is observed at the secondary nozzle sensor location. Figure 13 also shows that a second pressure rise and peak occurs almost out of phase with the disturbance applied at the boundary. This pressure rise begins during the period when the disturbance applied at the secondary nozzle is at a low pressure. It then decreases as the applied disturbance pressure increases, before the primary peak rises and follows the applied disturbance.

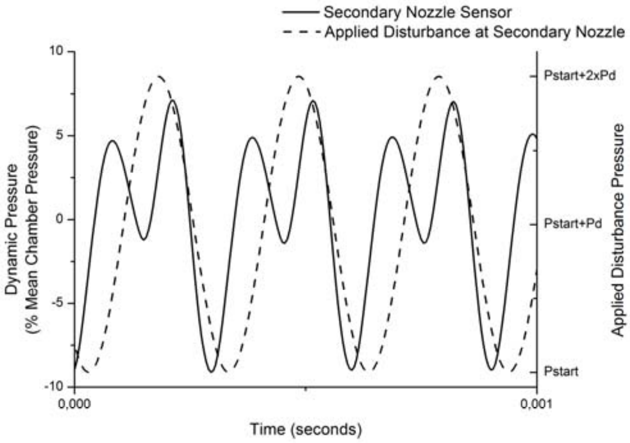

Figure 13: Extracted pressure data from the secondary nozzle sensor position during 1T mode excitation and the applied disturbance profile for the sinusoidal pressure boundary condition.

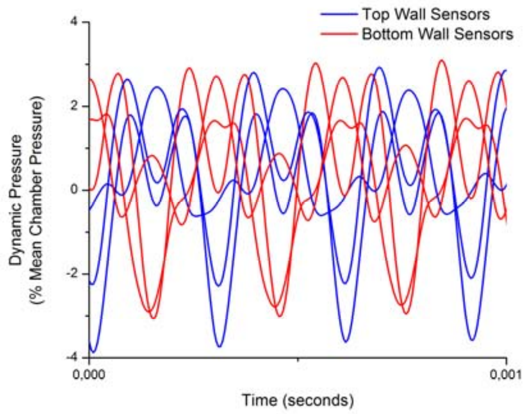

Figure 14: Extracted pressure data from the chamber wall sensor position during 1T mode excitation for the sinusoidal pressure boundary condition.

Figure 14 Shows simulated pressure data extracted from the wall mounted pressure sensor locations in the top and bottom of the chamber. The data extracted from unsteady simulations using the sinusoidal pressure boundary condition has significantly smaller amplitudes than that observed experimentally. The lower amplitude may be attributed to the maximum applied pressure which is insufficient to stagnate and halt the flow through the secondary nozzle, as would occur in reality. The wall sensors do not share a clear 1T mode phase relationship. The second peak observed in the secondary nozzle sensor position is out of phase with the imposed disturbance at the excitation frequency. The new disturbance profile does not match the desired excitation frequency and may instead prevent a 1T mode structure from developing.

6 Discussion

The structure of an acoustic mode is dependent on a number of factors other than the disturbance produced by the excitation system. Damping in the chamber also plays an important role in determining the mode structure. The current work has not considered if all sources of damping are being captured by the current model. Damping sources that could be considered in more detail include the influence of the injection feed system and viscous damping along the walls of the chamber. This will be addressed in future work.

The second rise in pressure in the secondary nozzle that is observed in the numerical results may correspond to the similar second rise in pressure observed experimentally (Figures 3 and 5). This pressure rise occurs when the exit pressure applied at the secondary nozzle exit plane is low. Further investigation of numerical results indicates that this rise in pressure occurs when the flow transitions to sonic in the secondary nozzle. Assuming istentropic flow the pressure at which flow from a volume at pressure P_0 through a nozzle will become sonic, known as the critical pressure P_{crit}, can be calculated via:

$$Pcrit = P_0 \left(\frac{2}{k+1}\right)^{k/(k-1)} \quad (2)$$

Where k is the specific heat ratio of the gas. During a cold flow experiment the combustion chamber pressure is approximately 30 bar. Considering the combustion chamber full of gaseous hydrogen at ambient temperature, the critical pressure is approximately 15.8 bar. Outside the secondary nozzle the pressure is approximately atmospheric, so that when the secondary nozzle is unobstructed by the teeth of the siren wheel the pressure is less than the critical pressure and the flow transitions to sonic. As the flow through the secondary nozzle is interrupted by the teeth of the siren wheel the pressure would increase and the flow through the nozzle would transition to subsonic. The pressure rise observed in the secondary nozzle sensor position may be the result of the flow transitioning to sonic flow through the secondary nozzle for part of the excitation period.

7 Conclusion

Methods for representing a secondary nozzle and siren wheel acoustic excitation system for simulating high frequency combustion instability experiments have been investigated. The investigation is motivated by the need to accurately reproduce the acoustic disturbance produced by the system without modelling the system in detail. Unsteady boundary conditions to represent the influence of the excitation system were applied to a model of the BKH combustor under cold flow operating conditions. The response of the model to each boundary condition was then analysed and compared to experimental data.

It has been observed experimentally that while the excitation system was intended to produce a sinusoidal disturbance, in reality it also excites overtones of the excitation frequency causing a steeper disturbance profile. A secondary pressure rise also occurs which may be due to the flow becoming sonic through the secondary nozzle for part of the excitation period. Although the disturbance produced does not match the intended sinusoidal disturbance, when operating at the 1T resonant frequency the pressure distribution recorded from wall mounted sensors in the chamber corresponds to a 1T mode structure.

The boundary conditions applied to represent the excitation system in this work did not reproduce the experimentally observed disturbance. The open/closed boundary condition produced a mode structure resembling the 1T mode, but also excited a number of overtones. The sinusoidal pressure boundary condition produced a mode shape that did not resemble the 1T mode. Overtones and secondary frequencies that are produced by the boundary conditions appear to have interfered and prevented a 1T mode from being established.

The boundary conditions that have been applied are relatively simple and have not been optimized for the BKH experiments. The applied boundary conditions will be modified to produce a disturbance that more closely matches the disturbance observed experimentally in future work. This initial experimentation has identified a number of phenomena that should be considered when using boundary conditions to represent a secondary nozzle and siren wheel excitation system.

Acknowledgments

This work is conducted within the scope of the DLR Pro-Tau project. The authors would like to thank Samuel Webster for helpful conversations and management of the BKH experiments, along with Dimitry Suslov, Mike Zeimßen and the members of the P8 test bench. The authors would also like to thank Bernd Wagner, Sebastian Karl, Volker Hannemann, and the members of the Aerodynamics and Flow Technology group at DLR Göttingen for the continued support and expertise provided.

Research undertaken for this report has been assisted with a grant from the Sir Ross and Sir Keith Smith Fund (Smith Fund) (www.smithfund.org.au). The support is acknowledged and greatly appreciated. The Smith Fund by providing funding for this project does not verify the accuracy of any findings or any representations contained in it. Any reliance on the findings in any written report or information provided to you should be based solely on your own assessment and conclusions. The Smith fund does not accept any responsibility or liability from any person, company or entity that may have relied on any written report or representations contained in this report if that person, company or entity suffers any loss (financial or otherwise) as a result.

References

[1] Beinke, S., Dally, B., & Oschwald, M, Modelling Acoustic Excitation for the Simulation of Combustion Instability Experiments, in: *18th Australasian Fluid Mechanics Conference,* Launceston, Tasmania, 2012

[2] Chehroudi, B., & Talley, D., Interaction of Acoustic Waves with a Cryogenic Nitrogen Jet at Sub- and Supercritical Pressures, in: *40th AIAA Aerospace Sciences Meeting & Exhibit*, Reno, Nevada, 2002.

[3] Chehroudi, B., Davis, D. & Talley, D., Initial results from a cryogenic coaxial injector in an acoustic field, in: *41st AIAA Aerospace Sciences Meeting & Exhibit, Reno, Nevada*, 2003.

[4] Gerhold, T., Friedrich, O., Evans, J., & Galle, M., Calculation of Complex Three-Dimensional Configurations Employing the DLR-TAU-Code, *AIAA paper 97-0167*, 1997.

[5] Hakim, L., Schmit, T., Ducruix, S. & Candel, S., Numerical simulation of cryogenic flames under high frequency acoustic modulation, *23rd ICDERS, Irvine, USA*, 2011.

[6] Hardi, J., Beinke, S., Oschwald, M. & Dally, B., Coupling Behaviour of Lox/H2 Flames to Longitudinal and Transverse Acoustic Instabilities, in: *48th AIAA/ASME/SAE/ASEE Joint Propulsion Conference & Exhibit,* Atlanta, Georgia, 2012.

[7] Hardi, J., Experimental Investigation of High Frequency Combustion Instability in Cryogenic Oxygen-Hydrogen Rocket Engines, PhD Thesis, The University of Adelaide, 2012.

[8] Hardi, J., Oschwald, M. & Dally, B., Acoustic characterization of a rectangular rocket combustor with liquid oxygen and hydrogen propellants, Proceedings of the Institution of Mechanical Engineers, Part G: *Journal of Aerospace Engineering*, 227: 3, 2013, 431-441.

[9] Harrje, D. T., and Reardon, F. H., (eds) Liquid Propellant Rocket Combustion Instability, *NASA SP-194*, 1972

[10] Karl, S. & Luedeke, H., Application of the DLR Tau code to predict acoustic damping rates in generic combustion chamber configurations, DLR IB 224 2012 A67, 2008.

[11] Laroche, E., Habiballah, M. & Kuentzmann, P., Numerical Analysis of Liquid Rocket Combustion Instability. Preliminary 3D Acoustic Calculations, in: *36th AIAA/ASME/SAE/ASEE Joint Propulsion Conference and Exhibit*, *Huntsville*, *Alabama*, 2000.

[12] Leocourt, R. & Foucaud, R., Experimetns on Stability of Liquid Propellant Rocket Motors, 23rd AIAA/SAE/ASME/ASEE Joint Propulsion Conference, San Diego, California, 1987.

[13] Mery, Y., Ducruix, S., Scouflaire, P. & Candel, S., Injection coupling with high amplitude transverse modes: experimentation and simulation, *C.R. Mecanique*, **337**, 2009, 426-437.

[14] Mery, Y., Hakim, L., Scouflaire, P., Vingert, L., Ducruix, S., & Candel, S., Experimental investigation of cryogenic flame dynamics under transverse acoustic modulations. *C.R. Mecanique*, **341**, 2013, 100-109.

[15] Nicole, A., Personal Communication, 13 August 2012.

[16] Nicole, A. & Habiballah, M., Numerical Analysis of Acoustic Instability, 4th International Conference on Launcher Technology “Space Launcher Liquid Propulsion”, Liege, Belgium, 2002.

[17] Nicole, A. & Habiballah, M., Investigations of some generic coupling mechanisms in high frequency combustion instability phenomenon – theory and numerical simulations, in: *44th AIAA Aerospace Sciences Meeting, Reno, Nevada*, **12**, 2006.

[18] Priem, J., guidelines for combustion stability specifications and verification procedures for liquid propellant rocket engines, *CPIA publication*, 1997

[19] Rey, C., Ducruix, S. & Candel, S., A method for the transverse modulation of reactive flows with application to combustion instability, Combustion Theory and Modelling, **9**, 2005, 5-22.

[20] Schmid, M. & Sattelmayer, T., Influence of pressure and velocity perturbations on the heat release fluctuations for coaxial GH2/GO2 injection,in: *4th European Conference for Aerosapce Sciences*, 2011.

[21] Schmid, M. & Sattelmayer, T., Interaction of Acoustic Pressure Fluctuations with Supercritical Nitrogen Jets, in: *48th AIAA/ASME/SAE/ASEE Joint Propulsion Conference & Exhibit, Atlanta, Georgia*, 2012.